Examination of Bone Chemical Composition in Osteoporosis Using Fluorescence-Assisted Infrared Microspectroscopy

LISA M. MILLER,[1] JYOTI TIBREWALA,[1] CATHY S. CARLSON[2]

Abstract. Although it is clear that osteoporosis is associated with a reduction in bone mass and a fragile skeleton, it is not understood whether the chemical composition of osteoporotic bone is different from normal bone. In this study, cynomolgus monkeys *(Macaca fascicularis)* were administered fluorochrome labels at one and two years after ovariectomy (Ovx) or Sham ovariectomy (Intact), that were taken up into newly remodeled bone. Using fluorescence-assisted synchrotron infrared microspectroscopy, the chemical composition of bone from Intact versus Ovx monkeys has been compared. Results from overall composition distributions (labeled + non-labeled bone) reveal similar carbonate / protein and phosphate / protein ratios, but increased acid phosphate content and different collagen structure in the Ovx animals. Analysis of the fluorochrome-labeled bone indicates similar degrees of mineralization in bone remodeled after one year, but decreased mineralization in Ovx bone remodeled two years after surgery. Thus, bone from monkeys with osteoporosis can be characterized as having abnormal collagen structure and reduced rates of mineralization. Coupled with factors such as trabecular architecture and bone shape and size, these ultrastructural factors may play a contributing role in the increased bone fragility in osteoporosis.

Introduction

Osteoporosis is a disease characterized by a reduction in bone mass and a skeleton that is more susceptible to fracture. However, studies have shown that there is an appreciable overlap in bone densities among normal individuals and those that sustain fractures, suggesting that low bone mass cannot solely explain the increased fracture rate in the aging population (World Health Organization, 1994). Although it is clear that bone mass is significantly reduced in osteoporosis, it is unclear whether bone remodeled after the onset of the disease differs in chemical composition from "normal" bone. This issue is extremely important because chemical composition influences the process of remodeling by affecting bone mineral crystal size, density, and solubility. Also, the fact that aged bone is more fragile suggests possible differences affecting bone strength and flexibility.

While the association of osteoporosis with estrogen deficiency is quite apparent, it is still not known how estrogen influences local regulation of bone remodeling (Erlebacher *et al*. 1995). For example, it is unclear whether bone remodeled before versus after menopause is chemically different. Increases in collagen synthesis and cross-link formation have been observed in monkeys with disuse osteoporosis (Yamauchi *et al*. 1988). Increased nonmineralized osteoid has been

shown in these monkeys as well (Mechanic *et al*. 1986). Recent IR microspectroscopic data have revealed differences in collagen maturity throughout normal trabeculae that are not detected in osteoporotic trabeculae. This variation is also observed across a normal osteon, but is absent from osteon in osteoporotic biopsies (Paschalis *et al*. 1999).

Since significant, irreversible bone loss can occur before physical symptoms appear in osteoporosis, it is important to study all ages and stages of the disease. Like post-menopausal women, ovariectomized female cynomolgus monkeys *(Macaca fascicularis)* develop osteopenia, with accelerated bone loss, high bone turnover rates, and reduced bone strength (Jerome *et al*. 1997). Six months after ovariectomy, bone turnover rates are 4-fold higher and spinal bone mineral densities are significantly lower in the ovariectomized monkeys as compared to the intact animals. Lower mineral densities demonstrate a deficit in bone formation with respect to bone resorption and increased turnover rates amplify this critical imbalance.

In our current work, we are using synchrotron IR microspectroscopy to compare (1) the mineral content, (2) protein content, and (3) mineral crystallinity of newly remodeled bone from ovariectomized versus intact female monkeys. In order to distinguish newly remodeled bone from old bone, the monkeys are administered

[1] National Synchrotron Light Source, Building 725 D, Brookhaven National Laboratory, Upton, NY 11973
[2] Department of Veterinary Diagnostic Medicine, College of Veterinary Medicine, University of Minnesota, 1333 Gortner Avenue, St. Paul, MN 55108

fluorochrome labels at various time points after ovariectomy. These drugs are then taken up into newly remodeled bone tissue and, using fluorescence microscopy, we are able to identify bone remodeled at known time points after ovariectomy. Figure 1 illustrates regions of (A) trabecular and (B) cortical bone remodeled at one (green) and two (orange) years after ovariectomy.

The fluorescent bands that signify regions of newly remodeled bone are only 5-10 μm wide. In order to achieve this type of spatial resolution with an IR microscope, a **synchrotron** IR source is necessary (Bantignies *et al*. 1998; Miller *et al*. 1998; Miller *et al*. 1997; Miller *et al*. 1999a; Miller *et al*. 1999b). At the National Synchrotron Light Source at Brookhaven National Laboratory, the brightness of IR light focused through a 10 μm pinhole is 100 times greater than a conventional IR source, improving the spatial resolution of the microspectrometer such that data can be rapidly collected with high signal-to-noise at the diffraction limit, which is 3-5 μm in the mid-IR region (Carr *et al*. 1995; Reffner *et al*. 1995).

Materials and Methods

ANIMALS: The tissues studied are from the female members of the cynomolgus monkey colony at the Comparative Medicine Clinical Research Center of the Bowman Gray School of Medicine. The animals were housed and fed identically for a minimum of two years and were randomized into 2 test groups: 1) Sham ovariectomized (Sham) and 2) Ovariectomized (Ovx). Bilateral ovariectomies were done on the monkeys in the Ovx group. One year after surgery, animal received calcein (10 mg/kg i.v.) on a 1 day label, 7 days off, 1 day label, 7 days off schedule.. Two years after surgery and 3 months prior to necropsy, animals received alizarin complexone (20 mg/kg i.v. on a 1-7-1-7 schedule.) These fluorochromes are taken up into newly remodeled bone and fluoresce green and orange, respectively, when exposed to UV light (see Figure 1).

Macroscopic measures of bone changes are available for all animals, including the proximal tibia, where our measurements are made. Bone mineral content (BMC) and bone mineral density (BMD) measurements of whole body and lumbar vertebrae, using dual-energy X-ray absorptiometry (DEXA), were performed at 6 month intervals. Knee joint radiographs and densitometry were done at yearly intervals. Serum assays were carried out every 3 months after surgery. Iliac bone biopsies were also collected at the time of ovariectomy or Sham ovariectomy, and from the contralateral ilium one year later. Two and a half years after ovariectomy or Sham ovariectomy, animals were
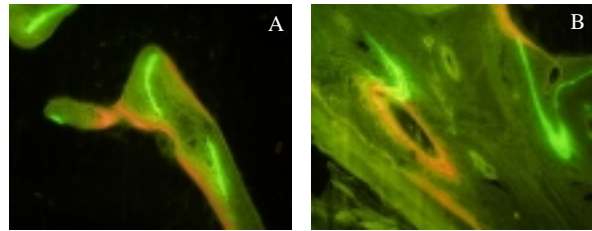
Figure 1. Fluorescence microscope images (100x magnification) of (A) trabecular and (B) cortical bone. Calcein-labeled bone (green fluorescence) was remodeled one year after ovariectomy and alizarin complexone-labeled bone (orange fluorescence) was remodeled two years after ovariectomy.

euthanized (Jerome *et al*. 1997) and the knee joints were collected for evaluation.

For all monkeys, the proximal tibia were collected at necropsy, serially sectioned, and microradiographed. The center section was embedded in methyl methacrylate/dibutyl phthalate. Two 5 μm-thick sections were cut from the tissue block using a sledge microtome fitted with a tungsten carbide knife; one was stained with toluidine blue (for enhanced optical imaging) (Carlson *et al*. 1996) and the second was left unstained (for IR microspectroscopy).

FLUORESCENCE MICROSCOPY: The unstained bone section is supported by placing it between two paper disks (13 mm dia. x 0.5 mm thick), each containing a narrow slit (2 x 5 mm). The region of interest is visible between the top and bottom slits. The sandwich assembly is mounted in a compression cell (Spectra Tech, Shelton, CT). An Olympus BX50 fluorescence microscope with 10x objective and U-MWB fluorescence cube is used to visualize the calcein (excitation: 495 nm, emission: 520 nm) and alizarin complexone (excitation: 570 nm; emission: 610 nm) fluorescent labels in the bone. Images are captured using a digital camera mounted on the microscope. Once the images are captured, the compression cell assembly is transferred directly to the IR microscope. More recently, an Olympus BX-FLA fluorescence accessory has been mounted to a Spectra Tech Continuμm IR microscope so that both fluorescence and IR images could be obtained simultaneously (Tague & Miller 1999).

INFRARED MICROSPECTROSCOPY: The common method for preparing bone samples for IR spectroscopy is by homogenization. However this procedure mixes all types of bone, making it nearly impossible to isolate particular types of bone, such as cortical or trabecular bone, for IR analysis. However, by putting IR light through a microscope equipped with special IR optics, IR micro-spectroscopy allows collection of IR spectra
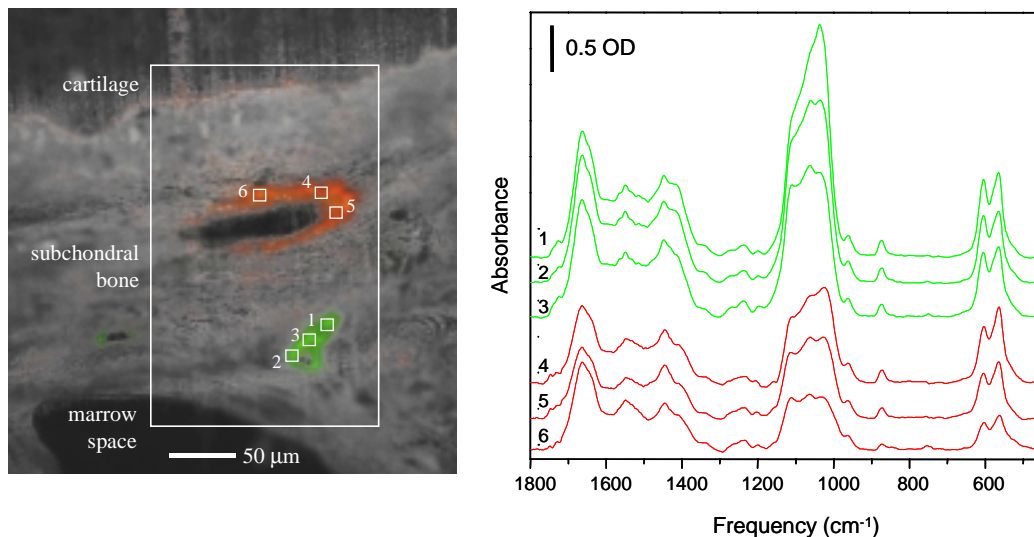
Figure 2. *(Left) Region of subchondral bone from an Intact monkey. An IR area map was collected within the region marked by the white box: 780 spectra were collected, 26 x 30 points, 20 x 20 μm square aperture, 20 μm steps, 64 scans per spectrum, 4 cm^{-1} resolution. (Right) Individual IR spectra were collected in the calcein-labeled region of bone (spectra 1-3) and alizarin complexone-labeled region of bone (spectra 4-6). For each of these spectra, 128 scans were collected at 4 cm^{-1} resolution using a 10 x10 μm square aperture and a Cu-doped Ge detector.*

from specific regions of normal and diseased states of bone as a function of age and morphology *in situ*.

IR spectra are recorded using a Spectra Tech Irμs Fourier Transform Infrared Microscope, equipped with a 32x Schwarzchild objective, motorized x-y stage and a Cu-doped Ge detector. The microscope is modified such that the conventional (globar) source is replaced by synchrotron IR light at Beamline U10B, The National Synchrotron Light Source, Brookhaven National Laboratory, Upton, NY. A camera is mounted to the microscope to enable optical imaging and recording of the areas investigated. Spectra are collected in transmission mode, 128 scans per point, 4 cm^{-1} resolution using *Atlμs* software (Nicolet Instruments). Area mapping is performed using 20x20 μm redundant apertures and 20 μm step size. Individual spectra collected from the fluorochrome-labeled regions of bone were performed using a 10x10 μm redundant apertures.

<u>DATA ANALYSIS:</u> Atlμs software is used to perform a baseline correction for each region of each spectrum. Then the Amide II (1595-1510 cm^{-1}), phosphate (500-650 cm^{-1}), and carbonate (905-825 cm^{-1}) bands are integrated to determine protein and mineral concentrations, respectively. Collagen structure is analyzed as a peak height ratio of 1660 / 1678 cm^{-1}. The acid phosphate / total phosphate content is calculated by measuring the peak height at 538 cm^{-1} and dividing by the total area under the ν_4 phosphate band (Miller *et al*. 1999c). Crystal size/perfection is determined as a ratio of stoichiometric (603 cm^{-1}) to non-stoichiometric phosphate (563 cm^{-1}) (Miller *et al*. 1999c). Once the

above-mentioned peak heights and areas are calculated, all of the results are expressed as ratios to correct for any variations in sample thickness. Once all ratios are calculated, frequency distributions are calculated using *Microcal Origin 6.0*. For the Intact animal distributions, 5 animals were examined for a total of ~1500 IR spectra. For the Ovx distributions, one animal was examined (440 IR spectra). Statistical difference analysis is performed using two-tailed t-tests at a 95% confidence level using *Minitab v12 for Windows*.

Curve-fitting of the Amide I band is used to investigate collagen structure. The curve-fitting is performed with *Grams 32* using a linear baseline and Gaussian peak-fit components. The number of components is defined by second derivative analysis. The frequency of each peak component is confined to ± 2 cm^{-1} from the second derivative position and peak widths are restricted to 20-30 cm^{-1}. Iterations are performed until the solution is converged and the correlation (R^2) is better than 0.995.

Results and Discussion

For the monkeys from which the tissues described here were collected, the Sham animals had significantly higher BMD and BMC values than the Ovx animals after two years (p<0.01) signifying the development of osteopenia in the Ovx group. Increased bone turnover, which accompanies estrogen deficiency, was also observed in the Ovx group; serum alkaline phosphatase (ALP), osteocalcin and tartrate-resistant acid phosphatase (TRAP), and the urinary deoxypyridinoline /
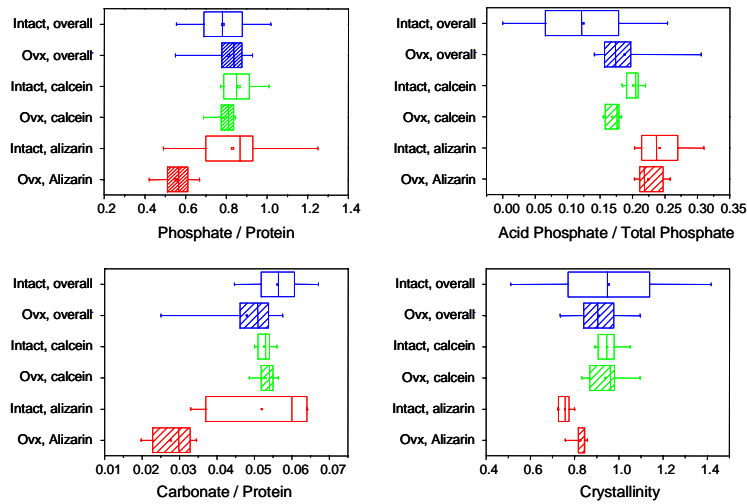
Figure 3. *Box and whisker plots illustrating the overall, calcein-labeled, and alizarin-labeled chemical composition distributions for Intact versus Ovx monkeys: (A) phosphate / protein ratio; (B) carbonate / protein ratio; (C) acid phosphate / total phosphate ratio; and (D) crystallinity. Ratios were calculated as described in the text. Box vertices represent 25, 50, and 75 percentiles of the data; whiskers represent 5 and 95 percentiles. Squares in the centers of the boxes represent the mean value for the distribution.*

creatinine (D-Pyr/Cr) ratio were all significantly increased in the Ovx relative to the Sham and nandrolone-treated animals (Jerome *et al*. 1997).

Figure 2 illustrates six spectra collected from newly remodeled bone in the tibial subchondral region of an intact monkey using 10x10 μm redundant apertures. Spectra 4-6 are taken from the region of orange fluorescence, which represents bone remodeled two years after ovariectomy and 3 months prior to necropsy. In these spectra, the protein intensity (e.g. 1650 cm^{-1}) is greater than the mineral intensity (e.g. 1050 cm^{-1}). The opposite is true for spectra 1-3, which were collected from the region of green fluorescence. This calcein-labeled bone was remodeled one year after ovariectomy and one year prior to necropsy. Thus, this latter bone had more time to mature before necropsy and is, therefore, more mineralized.

An area map was also collected from the same region of bone and is depicted by the white box in Figure 2

(*Left*). Box and whisker plots illustrating chemical composition distributions from this area map can be seen in Figure 3 (Intact, overall). The distributions were generated by calculating the phosphate / protein ratio, carbonate / protein ratio, acid phosphate / total phosphate content, and crystallinity for each spectrum. Distributions for the fluorochrome-labeled bone are also seen in Figure 3 (Intact, calcein & Intact, alizarin). The results confirm the findings from the individual spectra; they show (1) the mineral / protein ratios (both phosphate / protein and carbonate / protein) fall within the average distribution for the calcein-labeled bone (Intact, calcein), but are widely scattered with respect to the total distribution for the alizarin-labeled bone (Intact, alizarin), (2) the acid phosphate content is higher than the average distribution for both fluorochrome-labeled regions of bone, and (3) the average crystal size is larger for the calcein-labeled bone versus the alizarin-labeled bone, but both fall within the broad, overall distribution. All of these results are consistent and indicate that the bone labeled with calcein

	Intact, overall	Ovx, overall
Phosphate/protein	0.782 ± 0.142	0.812 ± 0.122
Carbonate/protein	0.0562 ± 0.0067	0.0480 ± 0.0101
Acid phosphate/ total phosphate	0.122 ± 0.0820	0.188 ± 0.0553
Crystallinity	0.958 ± 0.286	0.910 ± 0.109
Collagen structure	1.507 ± 0.131	1.400 ± 0.113

Table 1. *Chemical composition parameters (mean ± standard deviation) from entire subchondral bone areas (labeled and non-labeled bone included). Data for Intact animals were obtained from 10 area maps from six intact monkeys (~1500 spectra.) Data from Ovx animals were obtained from an area map from one ovariectomized monkey (440 spectra.)*

	Intact, calcein	Intact, alizarin	Ovx, calcein	Ovx, alizarin
Phosphate/protein	0.861 ± 0.0886	0.830 ± 0.256	0.792 ± 0.0571	0.554 ± 0.0849
Carbonate/protein	0.0527 ± 0.0022	0.0520 ± 0.0137	0.0530 ± 0.0028	0.0276 ± 0.0058
Acid phosphate/ total phosphate	0.201 ± 0.0129	0.242 ± 0.0409	0.168 ± 0.0122	0.225 ± 0.0223
Crystallinity	0.946 ± 0.0600	0.756 ± 0.0287	0.939 ± 0.0942	0.825 ± 0.0356
Collagen structure	1.248 ± 0.0460	1.222 ± 0.0278	1.392 ± 0.0373	1.198 ± 0.0972

Table 2. *Chemical composition parameters (mean ± standard deviation) from fluorochrome-labeled subchondral bone. For both the Intact and Ovx animals, six spectra were collected from each of the calcein- and alizarin complexone-labeled bone.*

(green fluorescence) is more mature that the bone labeled with alizarin complexone (orange fluorescence). Moreover, the calcein-labeled bone falls within the overall distribution (i.e. mature bone) for mineral / protein content and crystallinity, whereas the alizarin-labeled bone is immature compared to the average distribution. However it should be noted that for all of the labeled bone, the acid phosphate content is still higher than the average distribution. Several earlier infrared studies have also confirmed that acid phosphate content decreases as bone matures (Rey *et al*. 1989; Rey *et al*. 1990; Rey *et al*. 1991). This result suggests that, although the mineral content may be similar to mature bone (i.e. for calcein-labeled bone), the mineral *composition* is still different than the overall (average) distribution.

A similar area map was collected from a region of subchondral bone from an ovariectomized monkey (Miller *et al*. 1999b). Box and whisker plots illustrating the overall chemical composition distributions for this area
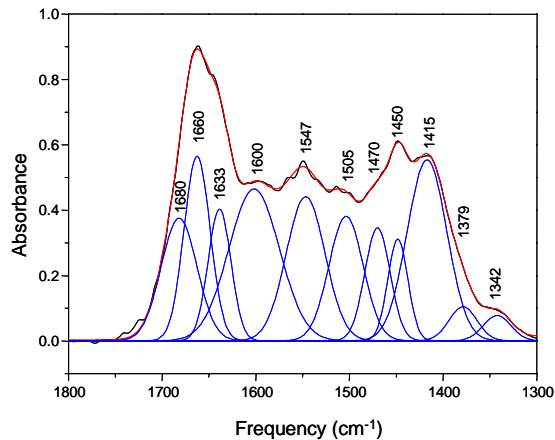

Figure 4. *Curve-fit analysis of the Amide I, II , and III region of an IR spectrum of bone. The Amide I band consists of three components: ~1680, 1660, and 1633 cm^{-1}. A ratio of the 1660 / 1680 cm-1 bands represents a measure of collagen cross-linking in bone (Paschalis, 1998).*

can also be seen in Figure 3 (Ovx, overall). The overall mineral / protein and crystallinity distributions are very similar for the Intact and Ovx animals. The average acid phosphate content is higher for the Ovx monkey than the Intact monkey, indicating a difference in mineral composition for the ovariectomized animal. Since acid phosphate content decreases as bone matures, it may be important to the interaction between bone mineral crystals and their environment (Wu *et al*. 1994). To date, the relationship between the inorganic crystal structure and the nucleation process induced by the organic matrix is still unclear. In this case, high acid phosphate content may be a marker of overall immature bone resulting from the increased bone turnover after ovariectomy.

Chemical composition distributions collected from calcein- (Ovx, calcein) and alizarin- (Ovx, alizarin) labeled bone from the Ovx monkey are also included in Figure 3. Both the acid phosphate content and average crystal size for the labeled bone are similar for the Intact and Ovx animals. Moreover, the acid phosphate content is higher and the average crystal size is smaller in the alizarin-labeled bone, both supportive of immature bone.

However unlike the Intact animals, the alizarin-labeled bone in the Ovx animal has mineral / protein ratios (phosphate / protein and carbonate / protein) that are considerably lower than the overall (average) distribution. Conversely, the calcein-labeled bone falls within the average distributions, similar to those regions probed in the Intact animal. Thus, bone remodeled one year after ovariectomy is similar to "normal" bone, but bone remodeled two years after ovariectomy is less mineralized than the alizarin-labeled bone from Intact animals. This result suggests a reduced rate of bone mineralization in the ovariectomized animal.

In addition to differences in mineral content in osteoporosis, significant evidence exists for differences in collagen content as well. For example, increased collagen synthesis, cross-link formation, and nonmineral-

ized osteoid have been observed in monkeys with disuse osteoporosis (Mechanic *et al.* 1986; Yamauchi *et al.* 1988). In addition, recent IR microspectroscopic data have revealed differences in collagen maturity across normal osteons which are absent from osteons in osteoporotic biopsies (Paschalis *et al.* 1999).

Since the protein content in bone is greater than 90% collagen, the Amide I band in a bone spectrum is representative of the collagen content and structure. Curve-fit analysis of the Amide I band reveals three bands, as can be seen in Figure 4. The highest frequency band at ~1680 cm^{-1} is sensitive to collagen cross-linking (Paschalis *et al.* 1998; Paschalis *et al.* 1999), whereas the 1660 and 1633 cm^{-1} bands are due to collagen secondary structure (Lazarev *et al.* 1985; Payne & Veis 1988). Thus, a plot of 1660 / 1680 cm-1 provides an inverse measure of the degree of collagen cross-linking with respect to overall collagen concentration (Paschalis *et al.* 1998). We have calculated the degree of collagen cross-linking for the Intact versus Ovx monkeys (Figure 5). As can be seen, the cross-linking is higher for the Ovx animal than the Intact animal, consistent with the results of Yamauchi, *et al.* (1988). Moreover, individual values from the fluorochrome-labeled bone indicate that collagen cross-linking is highest for the alizarin-labeled bone, but also high for the calcein-labeled bone with respect to the Intact overall distribution.

The strength of the collagen-mineral bonding and the quality/maturity of the collagen fibers are important to the mechanical behavior of bone (Boskey *et al.* 1999; Glimcher 1998) (and references therein). Poor bone quality is characteristic of numerous bone disorders, including osteogenesis imperfecta (OI). In a recent IR study by Boskey and coworkers, abnormal mineral and collagen properties were observed in mouse OI, which manifest themselves in fragile, brittle bones (Camacho *et al.* 1999). Conversely, increased mineralization in osteopetrosis leaves bone schlerotic and brittle (Boskey & Marks 1985). In both cases, it is not just the content of mineral and protein matrix in bone, but also the *composition* that is critical to the mechanical properties of bone.

Conclusions

By comparing the chemical composition of subchondral bone from intact versus ovariectomized monkeys, we find differences in both mineral composition and collagen structure. The overall (average) degree of mineralization is similar for Intact versus Ovx animals; however the mineral *compositions* vary. Specifically, the acid phosphate content in Ovx bone is higher than that from the Intact animals. In addition, collagen
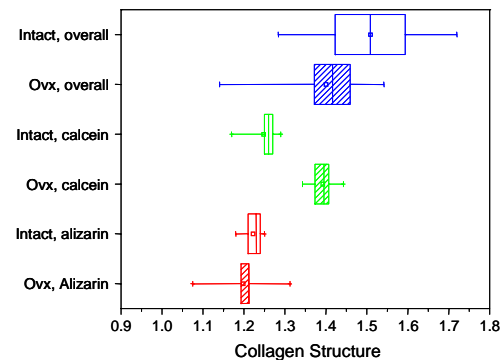

Figure 5. Box and whisker plots illustrating the overall, calcein-labeled, and alizarin-labeled collagen structure distributions for Intact versus Ovx monkeys. Ratios were calculated as described in the text. Box vertices represent 25, 50, and 75 percentiles of the data; whiskers represent 5 and 95 percentiles. Squares in the centers of the boxes represent the mean value for the distribution.

cross-linking is increased in bone from ovariectomized monkeys. This is consistent with biochemical findings by Yamauchi, *et al.* (1988) and recent IR microspectroscopic data from Paschalis, *et al.* (1999).

Examination of fluorochrome-labeled bone remodeled after ovariectomy versus Sham ovariectomy reveals reduced mineralization rates in the ovariectomized monkey. One year after ovariectomy, mineral / protein ratios are similar for Ovx versus Intact animals. However after 2 years, bone from the Ovx animal is less mineralized than the bone from the Intact animals. Although it is unclear how a reduced rate of mineralization is related to estrogen deficiency, this immature bone may signify a reduction in bone *quality*. Coupled with factors such as trabecular architecture and bone shape and size, other ultrastructural level factors may also play a contributing role in tissue properties. Specifically, the strength of the collagen-mineral bonding and the quality/maturity of the collagen fibers have been shown to affect mechanical behavior (Boskey *et al.* 1999). Therefore, ongoing studies are directed toward further analysis of the chemical composition of intact versus ovariectomized monkeys. In addition, analysis of hormone-treated animals may provide insight into how hormone replacement therapy affects the chemical composition of bone. By comparing the degree of mineralization, acid phosphate content, and collagen cross-linking in bone from intact, ovariectomized, and hormone-treated Ovx monkeys, we hope to develop a better understanding of the chemical basis for the remodeling imbalance and increased bone fragility in osteoporosis.

References

Bantignies, J. L., G. L. Carr, P. Dumas, L. M. Miller & G. P. Williams: Applications of Infrared Microspectroscopy to Geology, Biology, and Cosmetics. *Synchrotron Radiation News* 1998, **11,** 31-36.

Boskey, A. L. & S. C. Marks: Mineral and matrix alterations in the bones of incisor-absent (ia/ia) osteopetrotic rats. *Calcif. Tissue Int.* 1985, **37,** 287-292.

Boskey, A. L., T. M. Wright & R. D. Blank: Collagen and Bone Strength. *J. Bone Min. Res.* 1999, **14,** 330-333.

Camacho, N. P., L. Hou, T. R. Toledano, W. A. Ilg, C. F. Brayton, C. L. Raggio, L. Root & A. L. Boskey: The material basis for reduced mechanical properties in OIM mice bones. *J. Bone Min. Res.* 1999, **14,** 264-272.

Carlson, C. S., R. F. Loeser, C. B. Purser, J. F. Gardin & C. P. Jerome: Osteoarthritis in Cynomolgus Macaques III: Effects of Age, Gender, and Subchondral Bone Thickness on the Severity of the Disease. *Journal of Bone and Mineral Research* 1996, **11,** 1209-1217.

Carr, G. L., J. A. Reffner & G. P. Williams: Performance of an infrared microspectrometer at the NSLS. *Rev. Sci. Instr.* 1995, **66,** 1490-1492.

Erlebacher, A., E. H. Filvaroff, S. E. Gitelman & R. Derynck: Toward a molecular understanding of skeletal development. *Cell* 1995, **80,** 371-378.

Glimcher, M. J.: . In: *The nature of the mineral phase in bone: Biological and clinical implications.* Eds.: L. V. Avioli and S. M. Krane. Academic Press, San Diego, 1998, pp. 23-50.

Jerome, C. P., R. A. Power, I. O. Obasanjo, T. C. Register, M. Guidry, C. S. Carlson & D. S. Weaver: The androgenic anabolic steroid nandrolone decanoate prevents osteopenia and inhibits bone turnover in ovariectomized cynomolgus monkeys. *Bone* 1997, **20,** 355-364.

Lazarev, Y. A., B. A. Grishkovsky & T. B. Khromova: Amide I band of IR spectrum and structure of collagen and related peptides. *Biopolymers* 1985, **24,** 1449-1478.

Mechanic, G. L., D. R. Young & A. J. Banes: Non-mineralized and mineralized bone collagen in bone of immobilized monkeys. *Calcif. Tissue Int.* 1986, **39,** 62.

Miller, L. M., C. S. Carlson, G. L. Carr & M. R. Chance: A Method for Examining the Chemical Basis for Bone Disease: Synchrotron Infrared Microspectroscopy. *Cellular and Molecular Biology* 1998, **44,** 117-127.

Miller, L. M., C. S. Carlson, G. L. Carr, G. P. Williams & M. R. Chance: Synchrotron Infrared Spectroscopy as a Means of Studying the Chemical Composition of Bone: Applications to Osteoarthritis. *SPIE* 1997, **3153,** 141-148.

Miller, L. M., D. Hamerman, M. R. Chance & C. S. Carlson: Chemical Differences in Subchondral Osteoarthritic Bone Observed with Synchrotron Infrared Microspectroscopy. *SPIE* 1999, **3775,** 104-112.

Miller, L. M., R. Huang, M. R. Chance & C. S. Carlson: Applications of fluorescence-assisted infrared microspectroscopy to the study of osteoporosis. *Synchrotron Radiation News* 1999, **12,** 21-27.

Miller, L. M., V. Vairavamurthy, M. R. Chance, E. P. Paschalis, F. Betts, A. L. Boskey & R. Mendelsohn: *In Situ* Analysis of Mineral Crystal Size and Phosphate Environment in Bone using Infrared Microspectroscopy. *Biochim. Biophys. Acta, 2000,* submitted.

Paschalis, E., A. Ilg, K. Verdelis, M. Yamauchi, R. Mendelsohn & A. Boskey: Spectroscopic determination of collagen cross-links at the ultrastructural level, and its application to osteoporosis. *Bone* 1998, **23,** S342.

Paschalis, E. P., J. M. Lane, E. DiCarlo, F. Betts, R. Mendelsohn & A. L. Boskey: Organic matrix alterations in osteoporosis. *Connect. Tissue Res.* 1999, in press.

Payne, K. J. & A. Veis: Fourier transform IR spectroscopy of collagen and gelatin solutions: deconvolution of the amide I band for conformational studies. *Biopolymers* 1988, **27,** 1749-1760.

Reffner, J. A., P. A. Martoglio & G. P. Williams: Fourier Transform Infrared Microscopical Analysis with Synchrotron Radiation: The Microscope Optics and System Performance. *Rev. Sci. Instr.* 1995, **66,** 1298.

Rey, C., J. Lian, M. Grynpas, F. Shapiro, L. Zylberberg & M. J. Glimcher: Non-apatitic environments in bone mineral: FT-IR detection, biological properties and changes in several disease states. *Connect Tissue Res* 1989, **21,** 267-73.

Rey, C., M. Shimizu, B. Collins & M. J. Glimcher: Resolution-enhanced Fourier transform infrared spectroscopy study of the environment of phos-

phate ions in the early deposits of a solid phase of calcium-phosphate in bone and enamel, and their evolution with age. I: Investigations in the upsilon 4 PO4 domain. *Calcif Tissue Int* 1990, **46,** 384-94.

Rey, C., M. Shimizu, B. Collins & M. J. Glimcher: Resolution-enhanced Fourier transform infrared spectroscopy study of the environment of phosphate ions in the early deposits of solid phase calcium phosphate in bone and enamel and their evolution with age: 2. Investigations in the n_3 PO_4 domain. *Calc. Tissue Int.* 1991, **49,** 383-388.

Tague, T. & L. M. Miller: Development of an infrared microscope with fluorescence capabilities. *Microscopy Today 2000, 2, 26-32*.

World Health Organization: Assessment of fracture risk and its application to screening for postmenopausal osteoporosis. World Health Organization Study Group, Geneva, Switzerland, 1994.

Wu, Y., M. J. Glimcher, C. Rey & J. L. Ackerman: A unique protonated phosphate group in bone mineral not present in synthetic calcium phosphates. Identification by phosphorus-31 solid state NMR spectroscopy. *J Mol Biol* 1994, **244,** 423-35.

Yamauchi, M. M., D. R. Young & G. S. Chandler: Crosslinking and new bone collagen syntheses in immobilized and recovering primate osteoporosis. *Bone* 1988, **9,** 415.

Address Reprint Requests to:
Lisa M. Miller, Ph.D.
National Synchrotron Light Source, 725 D
Brookhaven National Laboratory
Upton, NY 11973-5000
lmiller@bnl.gov